

Pomeron-Reggeon relationship according to the topological expansion*

G. F. Chew and C. Rosenzweig[†]

Department of Physics and Lawrence Berkeley Laboratory, University of California, Berkeley, California 94720

(Received 21 July 1975)

The nature of the Pomeron and related effects are studied within the framework of Veneziano's topological expansion. At the second, or cylinder, level it is found that no new poles are generated but that first-level (planar) poles with $I = 0$ are shifted by the cylinder, the shifts being in opposite directions for positive and negative charge conjugation. The planar f , in particular, is shifted upward and may be interpreted near $t = 0$ as the Pomeron—with couplings lying roughly midway between the ideal mixing of a planar f and an SU_3 singlet. The Pomeron intercept and couplings (mixing coefficients) together with corresponding intercepts and couplings for ω , f' , and ϕ are semiquantitatively related through a single parameter to the properties of $\rho-A_2$. In the positive- t physical-particle region corresponding relations successfully correlate the breaking of the Iizuka-Okubo-Zweig rule to the ρ - ω mass difference. Comparison of the cylinder shift in this large- t region to that near $t = 0$ reveals the phenomenon of "asymptotic planarity"—the cylinder perturbation dying out rapidly with increasing t . It is pointed out that the small Pomeron slope as well as certain physical effects attributed in field theory to asymptotic freedom are consequences of asymptotic planarity.

I. INTRODUCTION

The duality-diagram topological expansion recently proposed by Veneziano¹ provides a potential basis for understanding previously obscure aspects of hadron dynamics, including the constellation of effects surrounding the term "Pomeron". Veneziano discovered a small dimensionless parameter related to the number of conserved internal hadronic quantum numbers that allows the hadronic S matrix to be topologically decomposed—in such fashion that successive levels of increasing topological complexity are plausibly of decreasing importance. The phenomenon characterized by the term "Pomeron" is absent from the first level but promises to appear at the second. Although the physical picture of the Pomeron given by the topological expansion is equivalent to the diffraction model of Chan, Paton, and Tsou,² the latter authors do not concern themselves with any motivating small parameter and ignore a variety of Pomeron-related second-level considerations. The object of the present paper is not only to elucidate the Pomeron but to identify other aspects of the hadronic S matrix that arise through the same topological second-level mechanism. An abbreviated account of some of our results has been given in Ref. 3.

Although the Pomeron discussed here is an approximate concept, it shares such a status with all other physically useful notions. The topological expansion, furthermore, provides a basis for assessing the accuracy of the approximation in terms of the motivating small parameter. This paper does not address the slippery question of whether the Pomeron intercept is exactly equal to 1 or what may be the strict mathematical struc-

ture of high-energy asymptotic limits. Such questions are inaccessible to physical measurement; physically answerable questions about the Pomeron all seem approachable through the topological expansion.

Veneziano has characterized the first level of his expansion by the term "planar" and the second by "cylinder"; we shall adhere to this terminology. The most interesting conclusion we reached is that cylinder poles correspond to shifted planar poles and not to a new set of singularities. The Pomeron and f trajectories, in particular, turn out to be one and the same. This unconventional identification, while clashing with some heretofore cherished notions, does not conflict with experimental facts. On the contrary, experiment supports the unified picture we achieve of the six leading trajectories ($f, \rho, A_2, \omega, f', \phi$) and their coupling—nondegenerate at the cylinder level but mutually related through a well-defined pattern. Our results together with those of Chan *et al.*⁴ are so successful with respect to experimental data and their theoretical motivation by Veneziano so attractive that we believe a major step forward in hadron physics is being realized.

In the next section we review essential features of the planar S matrix and proceed in Sec. III to establish an integral equation for the cylinder correction. Section IV shows how the cylinder shifts planar poles of both even and odd charge-conjugation symmetry without generating new singularities, features independently discovered by Schmid and Sorensen⁵ although interpreted by these authors as pathological. Section V deals with the qualitative behavior of the six leading planar trajectories affected by the cylinder, and Sec. VI discusses the qualitative viability of the proposed new pic-

ture for these trajectories with respect to currently available experimental information. Finally, in Sec. VII we employ a simple explicit model to emphasize the wealth of detailed physical content present in the cylinder. One striking outgrowth of this semiquantitative investigation is recognition of a connection with physical effects attributed in field theory to asymptotic freedom.

II. THE PLANAR S MATRIX

The Veneziano topological expansion begins with a planar approximation, defined through discontinuity formulas that can be graphically depicted in a plane. The idea of planarity enters in two ways. First of all, at this level of approximation the connected part itself is planar in the sense of Harari-Rosner^{6,7} duality diagrams. A five-line connected part, for example, is a sum of components each representable as shown in Fig. 1, where i, j, \dots are quark indices for internal quantum numbers. How many different values each index is allowed to take (i.e., how many different kinds of quarks need be included) and how much internal symmetry exists may be left as open questions, perhaps to be decided by the discontinuity formulas. The essential aspect of the quark lines is that they correspond to the boundary of an orientable two-dimensional surface. The reader is cautioned not to identify the planar approximation with the tree approximation to the dual resonance model—which ignores branch points in connected parts and keeps only poles. The planar S matrix is profoundly dependent on the discontinuities across its various branch cuts.

Where does the idea of a two-dimensional surface arise? We have here an example of the “which comes first (the chicken or the egg)?” logic that typifies bootstrap physics. *Some* information about the hadronic S matrix must be taken from experiment before analysis can begin, even though *all* aspects of the S matrix are supposed ultimately to be determined by requirements of self-consistency. Historically, Regge behavior and crossing led through finite-energy sum rules to duality and thence, with the additional information that

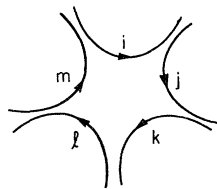


FIG. 1. Quark diagram representing one of the orderings for a five-line connected part. The indices i, j, \dots , are quark indices for internal quantum numbers.

low-mass hadrons have low internal quantum numbers (absence of exotics), to the Harari-Rosner two-dimensional diagrams. Later, however, Veneziano¹ found an *a posteriori* explanation for the relatively small magnitude of nonplanar S -matrix components, relating this smallness to the existence of conserved internal hadronic quantum numbers. (Veneziano employed a perturbative framework for his reasoning that started from a two-dimensional topology.) Although it remains to be seen whether discontinuity formulas demand the presence of internal quantum numbers, such a requirement is not out of the question. The resemblance between the planar S matrix and the observed hadronic world may thus ultimately emerge as a necessary consequence of self-consistency.

The second way in which planarity enters the picture—with more apparant dynamical content—is through the products that prescribe the discontinuities of planar connected parts. These products are planar in the sense of the example of a four-line connected-part discontinuity given in Fig. 2. The dots remind us that intermediate states in the bilinear products correspond to stable particles, while the plus and minus signs indicate the side of the cut on which the product member is to be evaluated. The essential character of the product—where there is no crossing of lines—might be characterized as “strong ordering.” It is important that planar discontinuities, so constructed, occur only in channels built from adjacent lines, corresponding to the famous “rubber sheet” property of the Harari-Rosner diagram which guarantees consistency between the (internal) spectrum of singularities and the entering (external) spectrum of particles. Since poles and normal thresholds occur only in channels with discontinuities, strong ordering limits such singularities to channels formed from adjacent lines. Also implied by “planar unitarity” is the exchange degeneracy of Regge singularities and thus the absence from the planar S matrix of an isolated, leading, even-charge-conjugation pole immediately identifiable as the Pomeron. Another important feature is the absence of Regge branch points, which do not arise until nonplanar discontinuity products enter at the subsequent levels of the topological expansion. We need consider Regge singularities no more complicated than poles. There is, however, no implication of strict linearity for Regge trajectories. The presence of normal threshold branch points precludes exact linearity.

Assuming amplitudes to be determined by their discontinuities (a key aspect of Regge asymptotic behavior), the solution, if any, of the nonlinear

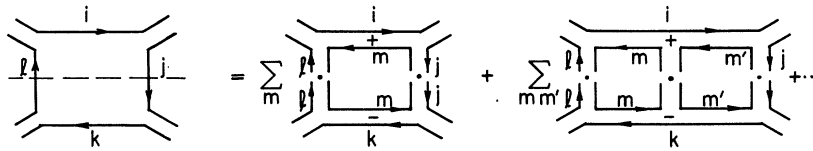


FIG. 2. An example of a planar four-line connected-part discontinuity. The dots remind us that intermediate states in the bilinear products correspond to stable particles, while \pm indicates the side of the cut on which the product member is to be evaluated.

planar discontinuity equations may be taken as a *definition* of the planar S matrix. Despite the absence of any proof that a solution exists, we are anticipating the above-enumerated general properties which any solution of the planar equations must possess.

The degree of arbitrariness permitted to the planar S matrix by its nonlinear constraining equations is a question of prime importance. For example, there is the question of how arbitrarily the internal quantum numbers may be assigned, or we may ask about the trajectory intercepts and residues (see Refs. 2 and 8–10). Despite their obvious importance these are not issues considered in the present paper, which concerns itself with the relation between the planar approximation and the first correction thereto. We make the assumption, following Veneziano, that the leading planar Regge poles bear a recognizably close correspondence with the two leading nonets of roughly exchange-degenerate physical trajectories (ρ, f, ω , etc.). The question to be studied here is how the Pomeron manifests itself in a systematic first correction to the planar approximation. More specifically, how is the Pomeron related to the leading planar trajectories? The answer to this question unavoidably has much to say about physical trajectories other than the Pomeron.

III. AN INTEGRAL EQUATION FOR THE CYLINDER CORRECTION TO THE PLANAR S MATRIX

The intermediate-state counting rules that justify the planar S matrix as a starting approximation lead to a comparably simple prescription for the

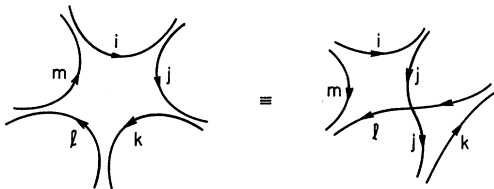


FIG. 3. A change in order of a five-line connected part represented by a twist.

first correction thereto. After the planar components, the next most important terms to include in a bilinear discontinuity product are those where matching changes of line ordering occur in the two members of a product. At this level of approximation each product member is itself planar and changes in order can be represented by a twist notation, as illustrated in Fig. 3. The first corrections to a planar discontinuity product such as that shown in Fig. 4 are then given by terms of the form in Fig. 5, the twists on the two sides of the “ladder” always matching in position. It is important to recognize that all such terms share the topology of a cylinder, although the twist notation is better suited to relations that must be expressed on a plane sheet of paper. We shall refer to the sum of all terms of the type shown in Fig. 5 as the “cylinder discontinuity.” That such an entity might be associated with the Pomeron in a dual unitarity scheme was proposed many years ago.^{11–15} The reader, however, is cautioned not to interpret pictures such as in Fig. 5 in the perturbative sense (eighth order in some coupling parameter) in which such diagrams have often been used in the past. Their meaning here derives only from topological considerations.

An essential aspect of the topological expansion is illustrated by the products in Fig. 5. Comparing to the planar product in Fig. 4 one sees that fewer intermediate states occur in the cylinder products in Fig. 5, the triple sum over internal indices having been reduced to a double sum. Provided that twists occur in matched pairs, one may easily verify that *any* cylinder product—independent of the number of twists—has *one* fewer sum

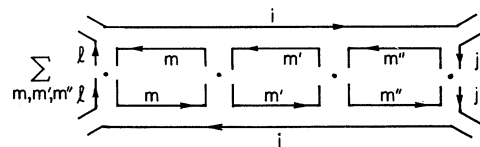


FIG. 4. A planar discontinuity product.

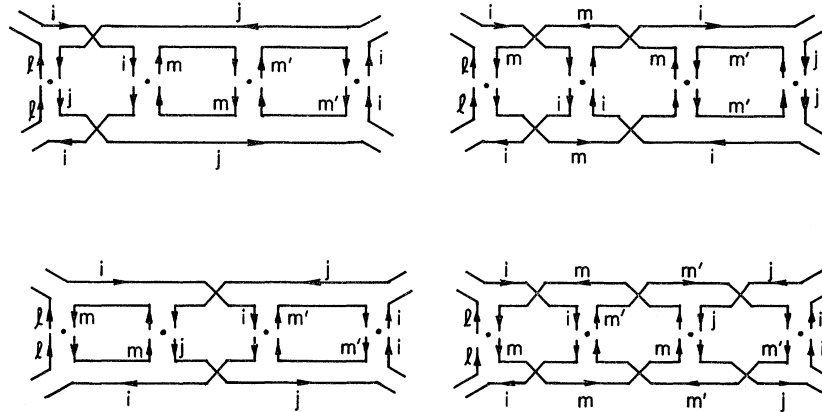


FIG. 5. Four examples of the first corrections to the planar discontinuity product shown in Fig. 4.

over internal indices than the corresponding planar product. The over-all cylinder discontinuity thus tends to be smaller than the planar discontinuity by a factor of the order of $1/N$, where N is the number of different values assignable to an internal index (i.e., the number of different quarks). Different values of the internal index contribute different proportions of the sums over intermediate states (e.g., index values carrying zero strangeness are quantitatively most important), so the $1/N$ estimate is not precise. With SU_N symmetry it can be shown that the cylinder couples only to the SU_N singlet; the $1/N$ factor then merely reflects the relative weight of this singlet representation. (We wish to thank G. Veneziano for correspondence about this point, which often causes confusion.) Veneziano showed that products more complicated topologically than the cylinder lose further sums over internal indices and should correspondingly be even smaller, the expected order-of-magnitude reduction factor being $(1/N)^m$ when m internal sums are lost.

Although any nonzero number of twist-pairs is topologically equivalent to a single twist-pair, a

meaning can be given to separate diagrams of the type shown in Fig. 5 by associating each in multiperipheral fashion with a region of phase space where the momentum transfer across each twisted link is small. If the major contribution arises from such regions—without important overlap—the complete cylinder discontinuity may be schematically represented as the series in Fig. 6 if a meaning can be found for “sewing” together adjacent planar discontinuities across a pair of twisted links. It is plausible that the required meaning can be achieved through the helicity pole expansion that has been used to decompose inclusive cross sections, the twist merely replacing a Regge-link physical signature factor $e^{-i\pi\alpha} \pm 1$ by a factor 1. Chan *et al.*^{2,8} have, in fact, suggested that the successive individual terms of Fig. 6 be interpreted physically at $t=0$ as proportional to the partial cross sections for production of successive numbers of “multiperipheral clusters”—each cluster corresponding to a complete planar discontinuity. Although we shall not attempt in this paper to develop a detailed helicity-pole representation of the twisted links, we take for granted that such a representation can be found—making the series in Fig. 6 meaningful.

Given such an assumption we can transform our products into the J plane by standard projection techniques.^{16,17} An analogous problem has been solved for multi-Regge models, showing that each separate discontinuity in a chain of the type shown in Fig. 6 is to be evaluated at the common values of J and t attached to the entire chain. Since for the purposes of the present paper we do not need the detailed Regge-index labeling of the planar discontinuities, we refer the reader to Refs. 16 and 17 for examples of how the nondiagonal labels

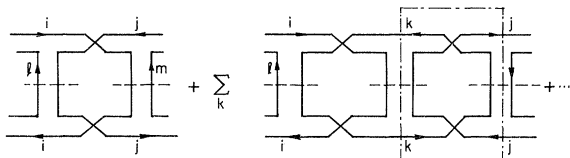


FIG. 6. A diagrammatic representation of the infinite series which generates the complete cylinder discontinuity of the four-line amplitude. The object contained within the dotted line box represents the cylinder operator C_1 .

may be chosen and then summed and integrated in forming the product of adjacent discontinuities. Although approximations are sometimes introduced in handling the phase space of multi-Regge models, the J -plane projection requires no approximation—resting on no more than Lorentz invariance. Such a projection makes easier the task of formulating an integral equation.

It may be seen from Fig. 6 that the cylinder communicates along its axis only with states carrying zero additive quantum numbers—states that may be classified by a single quark index together with an orientation. We may have, that is, either

$$\begin{array}{c} \xrightarrow{i} \\ \xleftarrow{i} \end{array} \text{ or } \begin{array}{c} \xleftarrow{i} \\ \xrightarrow{i} \end{array} .$$

As the quark arrows indicate, if two states are equivalent except for this orientation they are charge conjugates of one another. Introducing the notation of a twist operator C_1 corresponding to the box in the second term of Fig. 6, it follows that a single application of C_1 on a state of one orientation produces a superposition of states of the opposite orientation.

A planar discontinuity that participates in the cylinder chain is supposed to be decomposable into simple Regge poles; see Fig. 7 where the index γ labels the sequence of poles corresponding to quark type i . We may attempt to use these poles as the basis for a Hilbert space. Each such pole carries an orientation, even though in the planar S matrix the two orientations are equivalent (a manifestation of exchange degeneracy), and we have noted that the twist operator reverses the orientation. It is then natural to construct a space of states that are symmetric or antisymmetric combinations of the two orientations. The symmetric states are even under charge-conjugation ($C = +$) while the antisymmetric states are odd ($C = -$). The twist operator C_1 does not mix states of opposite charge-conjugation symmetry, and corresponding matrix elements of C_1 in the two subspaces have the same magnitude. The relative sign of C_1 is, however, opposite in the two sub-

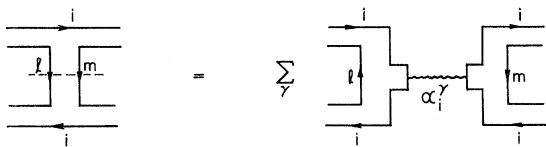


FIG. 7. The decomposition of a planar discontinuity into a sum over Regge poles. The index γ labels the sequence of poles corresponding to the quark type i .

spaces. That is,

$$C_1^- = -C_1^+ . \tag{3.1}$$

Using planar Regge poles (of well-defined C) as a basis we are now in a position to formulate an integral equation for the cylinder correction to the planar S matrix. Focusing on the t channel (along the axis of the cylinder), the problem schematically is that of summing the series of Fig. 8, where it is understood that there are separate series for even and odd charge conjugation. By attaching appropriate residue factors at left and right and summing over planar poles, as in Fig. 7, the physical discontinuity may be constructed from the series in Fig. 8, but the analysis will be simplified if such “end effects” are deferred until the final stage of the calculation. The most essential questions concern the interior of the cylinder, not the ends.

Although the cylinder correction is constituted by all terms of Fig. 8 beyond the first, it is convenient to study the sum of planar and cylinder contributions, i.e., the entire series. Thinking of linear operators in the space of planar Regge poles, at fixed values of J and t as well as definite charge conjugation, the leading term of Fig. 8 may be described as a diagonal “propagator” and designated by the symbol P . (P suggests both “planar” and “propagator.”) Assuming the kernel $C_1 P$ to be Fredholm (acting on an arbitrary state, it leads to a normalizable superposition of states), the entire series may be written as an integral equation

$$\begin{aligned} A &= P + PC_1 P + PC_1 PC_1 P + \dots \\ &= P + PC_1 A , \end{aligned} \tag{3.2}$$

with the formal solution,

$$A = (P^{-1} - C_1)^{-1} . \tag{3.3}$$

Even though this closed form is only schematic, it facilitates an extremely important inference to which we now turn attention.

IV. SHIFT OF PLANAR POLES COMMUNICATING WITH THE CYLINDER

Where are the poles of A —the sum of planar and cylinder components? To approach this question let us split the space based on planar poles into two subspaces according to a criterion of “communication” with the twist operator. Combining the two indices i and γ into a single index n and designating a planar basis state by $|n\rangle$, we define a superposition $|k\rangle$ of basis states as non-communicating if $C_1 |k\rangle = 0$. (For example, when there is SU_N symmetry, the only irreducible representations that communicate are SU_N singlets.)

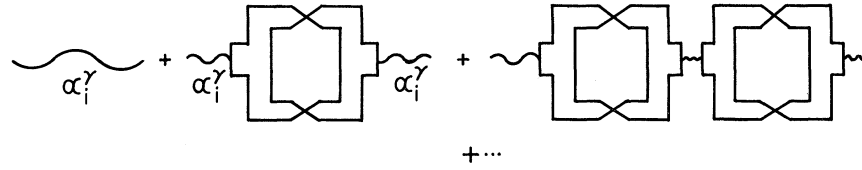


FIG. 8. The series representing the sum of the planar Regge pole α_i^γ plus the cylinder correction thereto. The series is formally summed via the integral Eq. (3.2).

By a standard procedure two complementary subspaces may then be identified, one containing only noncommunicating states while, within the other, all possible superpositions communicate with C_1 . Within the former subspace the cylinder has no effect and $A=P$, while within the latter subspace C_1 has no zero eigenvalues and thereby possesses an inverse.

By construction the planar poles reside in the propagator P while the twist operator C_1 , built from planar residues, contains no poles. Within the noncommunicating subspace the poles of A are evidently the same as the planar poles of P , but in the communicating subspace Eq. (3.3) tells us that planar poles are uniformly absent from A . That is, P^{-1} tends to zero (i.e., to the null operator) as $J \rightarrow \alpha_n$ so A tends to the finite limit $-C_1^{-1}$. In other words, the cylinder correction annihilates all planar poles that communicate with the cylinder.

At the same time the sum A develops new poles at points where

$$\det(1 - C_1 P) = 0, \quad (4.1)$$

and by examining the limit of small C_1 one finds the familiar quantum-mechanical adiabatic rule that the new poles are in one-to-one correspondence with the original planar poles. The cylinder thus may be considered as a perturbation that shifts those planar poles with which it communicates, without generating new poles.

It is straightforward, in fact, to derive from (4.1) a familiar-looking perturbation expansion for the shift of a trajectory originally at α_n :

$$\Delta\alpha_n = \langle n | C_1 | n \rangle + \sum_{n' \neq n} \frac{\langle n | C_1 | n' \rangle \langle n' | C_1 | n \rangle}{\alpha_n - \alpha_{n'}} + \dots \quad (4.2)$$

Here we mean by $|n\rangle$ a state in the cylinder-communicating subspace—which may be a superposition of the original planar states if there is degeneracy of the latter. Note that because $C_1^- = -C_1^+$ the first-order shift of an even charge-conjugation trajectory is opposite to that of the corresponding odd charge-conjugation trajectory although, to the extent that second- and higher-order

terms in the expansion (4.2) are appreciable, there will be an asymmetry in the magnitudes of upward and downward shifts. In any event, exchange degeneracy is lifted.

At the same time that the cylinder shifts the position of a planar trajectory there will be a modification of residue. In the original planar basis the residue matrix for each pole is (by construction) of the form

$$\langle n'' | R_n^P | n' \rangle = \delta_{n''n} \delta_{n'n}. \quad (4.3)$$

After the cylinder shift, the residue of each pole is still factorizable:

$$\langle n'' | R_n | n' \rangle = g_{n''n}^n g_{n'n}^n, \quad (4.4)$$

but a mixing has been introduced—given to lowest order by the familiar-looking formula

$$g_{n'n}^n \approx \frac{\langle n' | C_1 | n \rangle}{\alpha_n - \alpha_{n'}}. \quad (4.5)$$

In Sec. VII we discuss a nonperturbative calculation of the shifts in trajectory and residue when the cylinder coupling between only a small number of planar poles is included. Near $t=0$ the shifts turn out to be sufficiently large that it is worth going beyond the lowest order of a weak-coupling expansion but the qualitative picture at $t=0$ can still be described as a perturbation. In any event the magnitude of the cylinder shift depends upon t and, as discussed below, the shift becomes extremely small for $t \gtrsim 1 \text{ GeV}^2$. The one-to-one connection between shifted and unshifted poles is therefore guaranteed to be unambiguous if traced to the region where physical particles appear on Regge trajectories.

V. THE LEADING PLANAR TRAJECTORIES AND THEIR CYLINDER SHIFTS

For t near 0 and $0 \lesssim J \lesssim 1$ it is believed that for each charge conjugation there exist three planar trajectories. These correspond to the conserved internal quantum numbers, electric charge and strangeness, a possible way of attaching the quark index i to the quantum-number combinations being

as follows:

| i | Q | S |
|-----|-----|-----|
| 1 | 0 | 0 |
| 2 | 1 | 0 |
| 3 | 0 | 1 |

Nothing is gained by employing fractional charge and strangeness so long as we do not attempt to consider baryon number. Making integral assignments may help to emphasize that the boundary lines of dual diagrams are not equivalent to the quarks in naive models. To understand the experimental significance of the cylinder shift of these trajectories, it is essential to consider SU_2 and SU_3 symmetry, because it will turn out that the shift is larger than the breaking of SU_2 symmetry (at least near $t=0$) but smaller than SU_3 symmetry breaking. SU_2 symmetry makes $i=1$ equivalent to $i=2$ while SU_3 symmetry makes all three values of i equivalent to each other. For our purposes it is appropriate to impose the former condition but not the latter.

Labeling the three leading planar trajectories by the quark index $i=1, 2, 3$, those two corresponding to $i=1$ and 2 (no strange quark) will thus be taken as degenerate at $\alpha_0(t)$, while the third (strange quark) trajectory will be designated as $\alpha_3(t)$. Symmetric and antisymmetric combinations of $i=1$ and $i=2$ correspond to $I=0$ and $I=1$, respectively, and since, with SU_2 symmetry of pole residues, the twist operator C_1 is symmetric under $1 \leftrightarrow 2$ interchange, the cylinder communicates only with $I=0$ and the $I=1$ trajectory undergoes no cylinder shift. Neglecting nonplanar shifts of order higher than the cylinder, we are then led to identify the planar trajectory $\alpha_0(t)$ with the physically observed exchange-degenerate ρ and A_2 trajectories. (We emphasize once again that planar trajectories are not required to be linear.) An unambiguous base is thereby secured—from which all shifts may be measured.

There is unfortunately no such direct way to fix $\alpha_3(t)$ (which is purely $I=0$). It is empirically observed, however—from the near degeneracy of ω and ρ masses, as well as f and A_2 masses—that for $t \geq 1 \text{ GeV}^2$ the cylinder shift is small. We may confidently assume, therefore, that the conserved ϕ and f' particles lie close to the (strange-quark) planar trajectory $\alpha_3(t)$, and one thereby finds an interval of about 0.4 in J between $\alpha_0(t)$ and $\alpha_3(t)$ in the region of moderate t , with the former (non-strange quark) trajectory lying higher. The origin of this substantial gap remains unknown, but the fact that $\alpha_3 < \alpha_0$ does not contradict any tenets of the topological expansion. Conceivably, the gap

may turn out to be a *consequence* of planar unitarity when the full content of this nonlinear and difficult-to-analyze constraint becomes understood. The fact that $\alpha_1 \approx \alpha_2$ simplifies our task and must be recognized in confronting the data but neither SU_2 nor SU_3 symmetry is essential to the topological expansion.

Let us now consider how the four leading $I=0$ planar trajectories—two of each charge conjugation—are shifted by the cylinder. Recall that the leading pair has a common trajectory $\alpha_0(t)$ —degenerate with the physical ρ - A_2 trajectory. The positive charge-conjugation member of this pair we call f while the negative charge-conjugation member we call ω , since the physical $f(2^+)$ and $\omega(1^-)$ particles lie close to $\alpha_0(t)$. Which goes up and which goes down as a result of the cylinder shift?

At $t=0$ the positive definiteness of the discontinuity products from which we started translates unequivocally into an *upward* displacement for the leading trajectory of *even* charge conjugation. Thus f moves *above* ρ - A_2 while ω moves *below*, the upward displacement according to (4.2) being larger in magnitude than the downward. If SU_3 symmetry were exact, i.e., if $\alpha_3 = \alpha_0$, it can be shown that there would be no downward shift of the ω at all. This point is illustrated in Sec. VII. The shifted f at $t=0$ thus plays the role of the Pomeron, while the same cylinder mechanism that endows the Pomeron with its special prominence breaks ρ - ω degeneracy—pushing ω down, although not as far as f is pushed up.

What is happening to the pair of Regge poles,

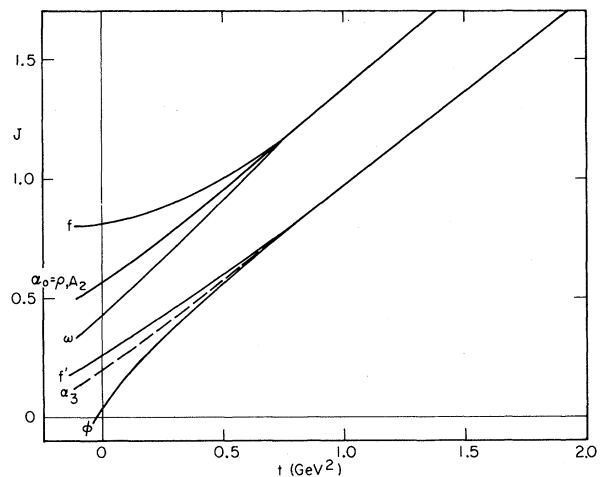


FIG. 9. The leading trajectory pattern after the cylinder correction has displaced the $I=0$ states. The scale of the $t=0$ splitting shown here is fixed by the choice $\alpha_0 - \alpha_3 = 0.37$, $\alpha_0 - \alpha_\omega = 0.14$.

f' and ϕ , associated with strange quarks, whose planar trajectory is $\alpha_3(t)$ —about 0.4 units of J below $\alpha_0(t)$? To the extent that SU_3 symmetry has any meaning (see Sec. VII), the even charge-conjugation trajectory is again shifted upward. Thus we expect the physical f' to lie above α_3 and the physical ϕ to lie below, the over-all descending order of the six leading trajectories being f , ρ - A_2 , ω , f' , ϕ . A semiquantitative estimate of the various intercepts is given in Sec. VII. (See Fig. 9.)

The residues of the four $I=0$ poles are also modified by the cylinder. The mixing given by Eq. (4.5) means that the physical f (the Pomeron) will possess some strange-quark content, as does the physical ω , even though the planar f and ω are purely nonstrange. The ρ and A_2 trajectories, on the other hand, will continue to have purely nonstrange quark content, while f' and ϕ will acquire a nonstrange admixture into their predominantly strange-quark character. Detailed predictions are given in Sec. VII. Here we remark only that the couplings predicted for the physical f turn out to be entirely compatible with those observed for the Pomeron.

VI. VIABILITY OF THE POMERON- f IDENTITY

The identity of Pomeron and f is not commonly assumed in Regge phenomenology; the standard picture contains an f , exchange degenerate with ρ , ω , A_2 , plus a Pomeron whose intercept is about 0.5 units higher. Since the standard picture has worked well, the reader may be skeptical that the picture presented here can be experimentally viable. Although we have not investigated all possible confrontations with data, we draw comfort first of all from the extensive studies of Dash¹⁸ and collaborators¹⁹ who successfully fitted large quantities of moderate-energy scattering measurements with a single high-lying Regge vacuum-type trajectory. A recent analysis of total cross section data within the even more restrictive framework described in the following section of this paper gives us further encouragement. At the present time we are unaware of experimental facts that conflict with our picture, although, as explained in Appendix B, measurement of $\pi\pi$ total cross sections in the few-GeV region may distinguish our picture from the conventional one.

An important aspect of the detailed predictions in the following section (see also Ref. 3) is their compatibility with a set of Pomeron coupling rules proposed by Carlitz, Green, and Zee (CGZ)²⁰ and known as the “ f -dominated” Pomeron.²¹ These rules have been strikingly successful but their motivation as presented by CGZ left obscure

the status of the physical f . Our approach not only yields the CGZ rules while clarifying the posture of the f but gives a corresponding set of rules for all six leading trajectories. From the standpoint of *our* analysis, in fact, it might be appropriate to speak of a “ ρ -dominated Pomeron,” since physical Pomeron properties can in our model be predicted from those of the physical ρ . (We are indebted to Chan Hong-Mo for this remark.)

What is the relation between our picture and that given by the conventional weak-coupling expansion of dual resonance models (DRM)?^{22,23} The lowest order of the latter—the so-called tree approximation—has many features in common with the planar S matrix, while at the next order a nonplanar loop appears—with the topology of a cylinder. This nonplanar loop introduces a new singularity not present in the tree approximation, that tentatively has been identified with the Pomeron. How can we reconcile this conventional picture with that based on the topological expansion?

First of all, a weak coupling expansion is inadvisable according to considerations explored by Veneziano, Chan, and collaborators,⁸⁻¹⁰ who showed that unitarity together with Regge behavior determines the magnitude of the coupling. If arbitrarily weak coupling is excluded, results from the conventional expansion must be regarded with skepticism. Secondly, the new singularity that appears in the nonplanar dual loop has in all models to date been a pole only for an unphysical number of space-time dimensions. The pole intercept, furthermore, is at $J=2$, not $J=1$. In four dimensions the new singularity is a branch point lying well below 1. It is only an optimistic conjecture that, as the dual model improves, the loop singularity will not only survive but will have properties close to those of the physical Pomeron.

On the other side of the coin, we have here failed to prove that in the topological expansion new singularities do not arise at the cylinder level—having begged the question by assuming the cylinder kernel to be Fredholm. It is probable that an infinite sequence of Regge poles (daughters) is needed to satisfy the planar discontinuity conditions, and the nondiagonal variables in our integral equation (e.g., Reggeon helicities and masses) span an infinite domain; so there is room on several counts for new singularities to appear in the solution of the equation. We see no reason, however, for such singularities to appear near the top of the J spectrum. Since estimates of the upward shift of the f place its physical intercept in the neighborhood of $J=1$,⁴ and since the origin of this shift is precisely the unitarity (diffractive) mechanism associated with the Pomeron, we feel

identification of Pomeron with f to be compelling.

We remark finally that if, after all, a brand new pole with vacuum quantum numbers is generated by the cylinder, it will be difficult to avoid a corresponding (even though lower-lying) odd-charge-conjugation pole. This point has been discussed by Freund and Nambu,²⁴ who stress the necessity in the conventional picture of finding a particle like the ω but slightly more massive.

VII. A SIMPLE MODEL FOR THE CYLINDER

Having developed a technical framework for the cylinder level of the topological expansion and recognized the broad implications thereof, let us now take a more concrete look at the situation. The model described in this section employs two supplementary simplifications: (1) neglect of the influence on the leading six trajectories from lower-lying trajectories, and (2) assumption of SU_3 symmetry for the matrix elements of the twist operator C_1 between the six leading states.

The accuracy of the first assumption—that of nearest-neighbor dominance—can ultimately be checked, since all matrix elements of C_1 are determinable from the planar S matrix. We have, in fact, identified and will discuss elsewhere certain interesting influences on leading trajectories by trajectories lying just below the top six, but we have found nothing to undermine the familiar phenomenon that the greatest influence on a state arises from nearest neighbors. The second assumption—assigning all SU_3 -symmetry breaking to the planar propagator via the difference between α_0 and α_3 —is based on the belief that planar Regge-pole residues should be relatively more symmetric than are pole positions. The corresponding assumption in Breit-Wigner data fitting has been strikingly successful—reduced widths showing substantially more accurate SU_3 symmetry than do resonance energies (masses). The difference between α_0 and α_3 will inevitably induce some symmetry breaking in the matrix elements of C_1 , but the effect is less important than in P —where all J singularities have been concentrated. For the $I=0$ subspace we then have

$$P^\pm = \begin{pmatrix} \frac{1}{J-\alpha_0} & 0 \\ 0 & \frac{1}{J-\alpha_3} \end{pmatrix}, \quad C_1^\pm = \pm k \begin{pmatrix} 2 & \sqrt{2} \\ \sqrt{2} & 1 \end{pmatrix}, \quad (7.1)$$

where α_0 , α_3 , and k are each functions of t , while

for the noncommunicating $I=1$ subspace

$$P^\pm = \frac{1}{J-\alpha_0}, \quad C_1^\pm = 0. \quad (7.2)$$

The leading six trajectories are thus described by three parameters at each value of t . The parameter k , as well as α_0 and α_3 , is determined by the planar S matrix (e.g., from planar triple-Regge couplings) and has in effect been so calculated at $t=0$ in Ref. 8, but we shall here regard k as a free parameter—to be fitted to experiment. As will be seen in Appendix B, our value at $t=0$ accords satisfactorily with the calculation of Ref. 8.

Readers experienced with multi-Regge dynamics may be puzzled by the absence from C_1 of factors $(J-\alpha_c)^{-1}$, where α_c is proportional to the sum of the helicities in the two-Reggeon connecting loop. It is necessary in this regard to remember that the planar amplitude in avoiding Regge cuts has zeros in triple-Regge vertices precisely arranged to cancel such singular loop factors. Exponential factors in the propagator P are sometimes included in multiperipheral models so as to represent threshold effects but when our model is expanded to encompass complex poles in the planar Regge spectrum, we automatically will be taking threshold effects into account. The inconsistency of including an exponential factor in P would then be apparent. Our neglect of threshold complications may thus be viewed as compatible with our particular truncation of the planar spectrum. To summarize, we believe that the simple J dependence taken in (7.1) is defensible.

The model embodied in (7.1) and (7.2) may be viewed as a refined version of a model proposed several years ago by Lee.¹¹ Our improvements are (1) recognition of the cylinder as the second level in a systematic expansion, (2) avoidance of unnecessary and unjustifiable kinematic approximations of the Chew-Pignotti type, by working in the J plane, and (3) inclusion of SU_3 -symmetry breaking. Point (1) allows us to see that awkward terms in the discontinuity product, neglected by Lee without justification, in fact correspond to a level of the topological expansion beyond the cylinder and are correspondingly smaller by factors $1/N$. We furthermore separate the simple perturbative problem of the cylinder shift from the far more difficult bootstrap calculation of planar parameters. In Lee's model the planar and cylinder levels were treated as parallel.

It is straightforward to solve the integral equation (3.2) with the simple forms (7.1). The reader will recognize our problem is that of diagonalizing a 2×2 mass matrix in the presence of an interaction. Shifts in trajectories are equivalent to shifts

of masses, and one finds two new even charge-conjugation eigenvalues corresponding to the trajectory positions

$$\alpha_{f,f'} = \frac{1}{2} \{ \alpha_0 + \alpha_3 + 3k \pm [(\alpha_0 - \alpha_3 + k)^2 + 8k^2]^{1/2} \}, \quad (7.3)$$

while the two new odd charge-conjugation trajectories (ω and ϕ) are given by a similar formula with k replaced by $-k$. It is easy to verify that if k is small compared to $\alpha_0 - \alpha_3$, expanding (7.3) yields

$$\begin{aligned} \alpha_f &= \alpha_0 + 2k + \frac{2k^2}{\alpha_0 - \alpha_3} + \dots, \\ \alpha_{f'} &= \alpha_3 + k - \frac{2k^2}{\alpha_0 - \alpha_3} + \dots. \end{aligned} \quad (7.3')$$

in accord with the perturbation formula (4.2), whereas in the limit where $\alpha_0 - \alpha_3$ is small compared to k one has

$$\begin{aligned} \alpha_f &\approx \frac{1}{3}(2\alpha_0 + \alpha_3) + 3k, \\ \alpha_{f'} &\approx \frac{1}{3}(\alpha_0 + 2\alpha_3). \end{aligned} \quad (7.3'')$$

The corresponding formulas for the odd charge-conjugation trajectories are

$$\begin{aligned} \alpha_\omega &= \alpha_0 - 2k + \frac{2k^2}{\alpha_0 - \alpha_3} + \dots, \\ \alpha_\phi &= \alpha_3 - k - \frac{2k^2}{\alpha_0 - \alpha_3} + \dots \end{aligned} \quad (7.4)$$

for weak cylinder coupling and

$$\begin{aligned} \alpha_\omega &\approx \frac{1}{3}(\alpha_0 + 2\alpha_3), \\ \alpha_\phi &\approx \frac{1}{3}(2\alpha_0 + \alpha_3) - 3k \end{aligned} \quad (7.4')$$

for cylinder couplings larger than SU_3 -symmetry breaking.

Although at first sight it looks strange in the latter case that α_ω and $\alpha_{f'}$, not only are equal but are independent of k , we recall that with SU_3 symmetry the cylinder couples only to SU_3 singlets. It is easy to show that in the symmetry limit ω and f' become members of octets and so do not communicate with the cylinder. In the same limit f and ϕ become pure singlets and communicate maximally. The important fact that f moves up

further than ω moves down may be attributed to these symmetry considerations or alternatively one may appeal to the notion of level "repulsion" and observe that all lower trajectories tend to push up the highest trajectory. Since the self-induced shift of each even charge-conjugation trajectory is upward, the self and mutual shifts here reinforce, but for the leading trajectory of odd charge conjugation the self-shift and the mutual shift tend to cancel.

If we designate the original $I=0$ planar basis states by $|0\rangle$ and $|3\rangle$, corresponding to the trajectories α_0 and α_3 , respectively, the two new states of even charge-conjugation are

$$\begin{aligned} |f\rangle &= \cos\theta^+ |0\rangle + \sin\theta^+ |3\rangle, \\ |f'\rangle &= -\sin\theta^+ |0\rangle + \cos\theta^+ |3\rangle, \end{aligned} \quad (7.5)$$

where by straightforward calculation

$$\tan 2\theta^+ = \frac{\sqrt{8} k}{\alpha_0 - \alpha_3 + k}. \quad (7.6)$$

At the same time the odd charge-conjugation states $|\omega\rangle$ and $|\phi\rangle$ are given by corresponding formulas with a mixing angle θ^- determined from Eq. (7.6) with k replaced by $-k$. For many purposes the following alternative mixing-angle formulas are more convenient:

$$\begin{aligned} \tan\theta^+ &= \frac{\alpha_f - \alpha_0}{\sqrt{2}(\alpha_f - \alpha_3)} = -\frac{\sqrt{2}(\alpha_{f'} - \alpha_3)}{\alpha_{f'} - \alpha_0}, \\ \tan\theta^- &= \frac{\alpha_\omega - \alpha_0}{\sqrt{2}(\alpha_\omega - \alpha_3)} = -\frac{\sqrt{2}(\alpha_\phi - \alpha_3)}{\alpha_\phi - \alpha_0}. \end{aligned} \quad (7.7)$$

The foregoing form for $\tan\theta^+$ corresponds to that proposed by Carlitz, Green, and Zee if one understands α_f to be their Pomeron trajectory, while α_0 and α_3 are the trajectories which they called f and f' .²⁰

Following CGZ we may use Eqs. (7.7) (see Appendix A) to compute ratios of various Reggeon-particle couplings in terms of ratios of trajectory displacements. We present a representative sample of these ratios in Table I. Note that we are now able to calculate many more ratios of coupling constants, all with the same general form.

TABLE I. γ_a^x is the coupling of Reggeon x at the $\bar{a}a$ vertex.

| | $r_x \equiv \frac{\alpha_x(0) - \alpha_p(0)}{\alpha_x(0) - \alpha_3(0)}$ | | | |
|-------------------|--|------------------------------------|------------------------------------|---|
| Ratio | $\frac{\gamma_K^f}{\gamma_\pi^f}$ | $\frac{\gamma_\phi^f}{\gamma_f^f}$ | $\frac{2\gamma_K^f}{\gamma_\pi^p}$ | $\frac{2\gamma_K^\omega}{\gamma_\pi^p}$ |
| Formal expression | $\frac{1+r_f}{2}$ | r_f | $(1+r_f)\cos\theta^+$ | $(1-r_\omega)\cos\theta^-$ |

An illustrative numerical application of our simple model is presented in Appendix B where we review experimental facts about total cross sections, all of which are consistent with $k(t=0)$ lying between 0.1 and 0.2. Even this weak cylinder coupling is sufficient to give the f (Pomeron) a dominant position and to force its couplings to lie roughly midway between those of an SU_3 singlet and those of an "ideal" mixture like the physical f particle. Such a Pomeron might well be described as "schizophrenic" although not quite in the same sense as proposed by Chew and Snider.²⁵

Our simple model allows trajectory and coupling shifts to be determined by a single parameter at each value of t , not just at $t=0$. Thus, mass differences between physical particles (e.g., ρ and ω) allow the determination of k at appropriate nonzero positive values of t and Eqs. (7.7) become predictions for mixing angles (e.g., ϕ , ω , or f, f' mixing). (We have defined θ^\pm such that these angles are rotations toward zero away from the ideal quark mixing angle $\text{arccot}\sqrt{2}$.) We are thereby led to recognize that the symmetry-breaking phenomena discussed by CGZ at $t=0$ for the Pomeron is but one manifestation of a general mechanism which is also responsible for violation of the rule of Iizuka,²⁶ Okubo,²⁷ and Zweig²⁸ for *physical particles* (IOZ rule).

In Appendix B it is found that for $t \geq 1 \text{ GeV}^2$ the value of k lies between 0.01 and 0.02—much smaller than at $t=0$. We find this empirical fact striking. The phenomenon that as t becomes more positive the cylinder correction becomes smaller and the planar approximation better shall henceforth be referred to as asymptotic planarity. In principle this decrease in magnitude should be predictable from a knowledge of the planar S matrix (triple-Regge couplings), but no explicit calculation has yet been performed. We nevertheless draw encouragement from the following consideration: A small slope for the Pomeron trajectory at $t=0$ is implied by the rapid decrease of $k(t)$. That is to say, if the displacement of f (Pomeron) above ρ shrinks to a tiny magnitude by the time α_ρ reaches $J=1$, the height of α_f at $t=m_\rho^2$ cannot be much above its height at $t=0$ (see Fig. 9). Conversely, generation from the planar S matrix of the small Pomeron slope at $t=0$ implies a content within planar amplitudes that will produce a rapid decrease of $k(t)$ as t grows. The success of Ref. 8 in calculating the Pomeron slope is therefore encouraging to the prospect of understanding asymptotic planarity.

Many of the physical effects associated with the cylinder kernel have recently received attention in quark models where they are associated with gluons. Low²⁹ has proposed a model where the

Pomeron is conceived as arising from gluon exchange. Appelquist and Politzer³⁰ have discussed the validity of the IOZ rule also within the quark-gluon framework. We find it striking that both in the latter model and in our topological framework the validity of the IOZ rule depends on characteristic couplings becoming weaker as t (or m^2) increases. In the field theoretical approach gluon coupling constants become small (asymptotic freedom) while in the S -matrix approach cylinder couplings $k(t)$ become small (asymptotic planarity).

The prospect that physical effects attributed to gluons are to be understood through properties of the planar S matrix increases dramatically any estimate of the ultimate impact on particle physics by the topological expansion.

ACKNOWLEDGMENTS

We are grateful to numerous colleagues who have helped us through critical comments. We are especially indebted to Chan Hong-Mo and Gabriele Veneziano. The motivation for this study, in fact, arose from private communications with Dr. Veneziano.

APPENDIX A: CROSSING SYMMETRY AND PHYSICAL AMPLITUDES

As in standard DRM, the complete planar N -line connected part is obtained by summing over the $\frac{1}{2}(N-1)!$ inequivalent external line permutations of an ordered N -point function of the type shown in Fig. 1. (Two permutations are equivalent if related by a cyclic or an anticyclic permutation.) Similarly at the cylinder level, in order to satisfy crossing symmetry one must sum over several cylinder configurations, although in the text we concentrated on one discontinuity of a particular cylinder. We were justified in so doing insofar as we were studying individual Regge poles. Here we explain how physical crossing-symmetric amplitudes are to be constructed from the primitive planar and cylinder discontinuities discussed in the text. We begin with the construction of a physical three-Reggeon vertex, which will include the "end effects" referred to in Sec. III. In appropriate pole-dominant limits where branch points are unimportant, we are then in a position to construct physical connected parts.

Suppose we are given the (planar) coupling G_{abc}^P between three planar Regge poles. What is the corresponding coupling between cylinder-shifted poles? In terms of the cylinder mixing coefficients g_n^a , the answer is evidently

$$G_{abc} = \sum_{a'b'c'} g_{a'}^a g_{b'}^b g_{c'}^c G_{a'b'c'}^P, \quad (\text{A1})$$

a straightforward rule that accomodates the consistent cylinder renormalization of both "internal" and "external" particles. Crossing symmetry is assured.

The construction of the planar couplings G_{abc}^P for states of well-defined isospin and charge conjugation has been discussed recently in Ref. 5, which develops the relation between Chan-Paton factors and the quark-line boundaries of the planar dual diagram. We have nothing new to propose in this connection.

As an example of the use of (A1) let us consider the couplings that control the ratio of high-energy total cross sections of ω and ϕ . These would be $G_{\phi\phi f}$ and $G_{\omega\omega f}$, where each of the $\phi(\omega)$ trajectories is taken at $t=m_\phi^2(m_\omega^2)$ while the f (Pomeron) is taken at $t=0$. In the approximation of Sec. VII we have the following nonvanishing mixing coefficients to consider:

$$\begin{aligned} g_\omega^\omega &= g_\phi^\phi = \cos\theta^-, \\ g_\phi^\omega &= -g_\omega^\phi = \sin\theta^-, \\ g_f^f &= \cos\theta^+, \\ g_f^\omega &= \sin\theta^+. \end{aligned} \quad (\text{A2})$$

The corresponding nonvanishing planar couplings are $G_{\phi\phi f}^P$ and $G_{\omega\omega f}^P$, so from (A1) we have

$$G_{\phi\phi f}^P = \cos^2\theta^- \sin\theta^+ G_{\phi\phi f}^P + \sin^2\theta^- \cos\theta^+ G_{\omega\omega f}^P \quad (\text{A3})$$

and

$$G_{\omega\omega f}^P = \cos^2\theta^- \cos\theta^+ G_{\omega\omega f}^P + \sin^2\theta^- \sin\theta^+ G_{\phi\phi f}^P. \quad (\text{A4})$$

If SU_3 symmetry is assumed for the planar couplings, one has additionally the condition

$$G_{\phi\phi f}^P = \sqrt{2} G_{\omega\omega f}^P, \quad (\text{A5})$$

so

$$\frac{G_{\phi\phi f}}{G_{\omega\omega f}} = \frac{\sqrt{2} \cos^2\theta^-(t=m_\phi^2) \sin\theta^+(t=0) + \sin^2\theta^-(t=m_\phi^2) \cos\theta^+(t=0)}{\cos^2\theta^-(t=m_\omega^2) \cos\theta^+(t=0) + \sqrt{2} \sin^2\theta^-(t=m_\omega^2) \sin\theta^+(t=0)}. \quad (\text{A6})$$

To the extent that θ^- is negligibly small at $t=m_\phi^2$, m_ω^2 the ratio reduces to $\sqrt{2} \tan\theta^+(t=0)$ —the result of Carlitz, Green, and Zee. The ratios listed in Sec. VII are obtained in a similar fashion.

To construct an amplitude from discontinuities one must add the contribution from right and left cuts. Not surprisingly, when this is done for both cylinder and planar discontinuities one finds the usual signature factors for shifted Regge poles. For example, the f (Pomeron) contribution carries a factor $\exp(-i\pi\alpha_f)+1$, while the ω contribution carries a factor $\exp(-i\pi\alpha_\omega)-1$.

Cylinders along the s and u axes have not been considered here. With respect to the J plane for the t channel, these cylinders give rise to Regge-Regge cuts with the Finkelstein³¹ selection rules (allowing certain exotics), but such cuts lie below those singularities that have received attention in this paper.

APPENDIX B: PRELIMINARY CONFRONTATION WITH MODERATE-ENERGY DATA

For two different reasons we confine attention to moderate energies: (1) Terms beyond the cylinder in the topological expansion increase in importance with energy. Pomeron-Pomeron and Pomeron-Reggeon cuts, in particular, have not yet appeared by the cylinder level—carrying additional $1/N$ factors—but such cuts are nevertheless expected to increase in relative magnitude

with energy and ultimately to play a significant role. (2) Confinement of attention to the six leading trajectories ignores degrees of freedom like baryon number that go beyond charge and strangeness. At energies sufficiently high to excite such additional degrees of freedom the simple model of Sec. VII requires extension. In particular, the experimental fact that total cross sections begin to increase at higher energies is not representable by the six-trajectory model. Inclusion of additional high-threshold degrees of freedom, such as baryon number, can accommodate the rise without altering the moderate-energy prediction^{32,33} (the cylinder coupling with lower-lying trajectories can push the f above $J=1$), but before making a serious study of such threshold complications we thought it worthwhile and instructive to confront the simple model with moderate-energy data.

This preliminary analysis takes its parameters to accord with $\alpha_\rho(0)=0.57\pm 0.01$ and $\alpha_\omega(0)=0.43\pm 0.01$ as determined from total cross section differences between 4 and 200 GeV.³⁴ These intercepts are consistent with data confined to energies where baryon-antibaryon production is negligible, but the displacement $\alpha_\rho(0)-\alpha_\omega(0)$ is not accurately determined from such energies. This displacement we use to set the scale of the cylinder shift at $t=0$.

A first question is whether such a modest down-

ward shift of ω can be compatible with the substantial upward f -shift needed if the f is to be identified as the Pomeron. In this connection the precise value of $\alpha_3(0)$ is not crucial. Taking $\alpha_3(0) = 0.2$, together with $\alpha_0(0) = \alpha_\rho(0) = 0.57$, we find from Eq. (7.3) that $k(0) = 0.10$ is required to shift $\alpha_\omega(0)$ from 0.57 down to 0.43. Such a value for $k(0)$ moves $\alpha_f(0)$ up to 0.81. If we wish to move $\alpha_f(0)$ all the way from 0.57 up to 1.0, one requires $k(0) = 0.17$; the ω trajectory is then pushed down only to 0.39. Realizing that Dash and collaborators¹⁸ have been able to fit all available elastic and diffractive-dissociation data up to 30 GeV with a single vacuum trajectory of intercept 0.85, we are assured that a value of $k(0)$ somewhere between 0.10 and 0.20 can produce an adequately prominent Pomeron while at the same time giving the more modest ρ - ω displacement indicated by experiment.

There is at present no experimental evidence to support our prediction that ρ - A_2 degeneracy is less broken than ρ - f . Tests at $t=0$ based on total cross sections are consistent with ρ - A_2 degeneracy but are insensitive to trajectory shifts of the order 0.1. Data for $t < 0$ are expected theoretically to be more sensitive to Regge cuts and are found, in fact, to be incompatible with a simple Regge-pole description. The accuracy of ρ - A_2 degeneracy is therefore difficult to determine, either for $t=0$ or for $t < 0$.

A specific choice for k implies, by the considerations of Appendix A, definite ratios of Reggeon couplings to π and K . One finds, up to a common multiplicative factor,

$$\begin{aligned} \gamma_\pi^\rho &= 2, & \gamma_\pi^{A_2} &= 0, \\ \gamma_K^\rho &= 1, & \gamma_K^{A_2} &= 1, \\ \gamma_\pi^f &= 2 \cos \theta^+, & \gamma_\pi^{f'} &= -2 \sin \theta^+, \\ \gamma_K^f &= \cos \theta^+ + \sqrt{2} \sin \theta^+, & \gamma_K^{f'} &= -\sin \theta^+ + \sqrt{2} \cos \theta^+, \\ \gamma_\pi^\omega &= 0, & \gamma_\pi^\phi &= 0, \\ \gamma_K^\omega &= \cos \theta^- - \sqrt{2} \sin \theta^-, & \gamma_K^\phi &= -\sin \theta^- - \sqrt{2} \cos \theta^-. \end{aligned} \quad (\text{B1})$$

Certain of these ratios are reproduced in Table I in terms of the parameters

$$\begin{aligned} r_f &= \sqrt{2} \tan \theta^+ = \frac{\alpha_f - \alpha_\rho}{\alpha_f - \alpha_3}, \\ r_\omega &= \sqrt{2} \tan \theta^- = \frac{\alpha_\omega - \alpha_\rho}{\alpha_\omega - \alpha_3}. \end{aligned} \quad (\text{B2})$$

One may ask whether experiments on πN and KN total cross sections are compatible with these ratios when $k(0)$ has a value compatible with trajectory intercepts. A preliminary study by Stevens³⁵ has given an affirmative answer for energies between 4 and 30 GeV, extending the

check already made by CGZ for the most easily measured ratio γ_K^f/γ_π^f . [Stevens was able to fit $K^\pm p$ and $\pi^\pm p$ total cross sections over this moderate-energy interval with f, ρ, A_2, ω trajectories and residues that are compatible with the model of Sec. VII if $k(0) = 0.15$, $\alpha_0(0) = 0.57$, $\alpha_3(0) = 0.2$.]

It is well known that the qualitative behavior of exotic versus nonexotic total cross sections is nicely explained in terms of the conventional picture where a Pomeron with an intercept near $J=1$ is added to a set of exchange-degenerate trajectories. The difference between the present formulation of two-component duality (the background is dual to the full cylinder contribution, not just the Pomeron piece) and the traditional formulation can be described as the difference between the strong and weak versions of the Harari-Freund ansatz.

The strong Harari-Freund ansatz says that exotic cross sections are relatively flat—a statement which is a consequence of exact exchange degeneracy. The contribution from the Reggeons exactly cancel each other, leaving only the Pomeron of intercept approximately 1. The weak version of the ansatz requires only that total cross sections for nonexotic s -channel processes are larger than corresponding exotic cross sections. In our model we expect exotic cross sections to rise toward their asymptotic Pomeron-dominated behavior. For example, in $\pi^+\pi^+$ and $K^+\pi^+$ only the f and ρ trajectories contribute, with roughly equal strength but opposite sign. Since $\alpha_f(0)$ is significantly larger than $\alpha_\rho(0)$ even though still less than 1, we expect these cross sections to show a rising tendency at low energies that may provide a test capable of distinguishing the two different versions of the Harari-Freund ansatz.

If only the weak version holds how are we to explain the relatively flat pp and K^+p total cross sections? The explanation lies in the circumstance that these reactions involve a more complicated system of poles and residues. We refer the reader to the details of the K^+p fit³⁵ for an example of how the energy variation arising from different components can mutually compensate.

Suppose we continue our model to the positive- t region and apply it to the physical-particle mass differences between ρ and ω and between f and A_2 . These differences are sufficiently small that the first-order perturbation should be amply accurate, and the signs of the observed differences are as expected if $k(t)$ does not change sign, but the differences are so small that the finite width of resonances becomes a limitation. The complex mass is the position of the pole, whose real part may be shifted from the Breit-Wigner resonance “mass” quoted in the standard tables by a sub-

stantial fraction of the width. The best that can be done in the absence of more precise knowledge of the pole positions is a rough estimate that in this positive- t region $0.01 \lesssim k \lesssim 0.04$.

Even though the mass shifts are only crudely known, their small magnitude suffices to explain via Eqs. (7.7) the extraordinary validity of the

IOZ rule. If we turn the question around and ask for the magnitude of the cylinder coupling needed to explain the observed decay of the ϕ into non-strange particles, we find $k(t=m_\phi^2) \approx 0.02$. Details of this calculation will be presented in a separate paper³⁶ that considers a variety of physical phenomena related to asymptotic planarity.

*This work was supported in part by the U. S. Energy Research and Development Agency (ERDA) and in part by NSF under Contract No. MPS74-08175-A01.

†Present address: Physics Department, University of Pittsburgh, Pittsburgh, Pennsylvania 15213.

¹G. Veneziano, Phys. Lett. 52B, 220 (1974); Nucl. Phys. B74, 365 (1974).

²Chan H.-Mo, J. E. Paton, and Tsou S.-T., Nucl. Phys. B86, 479 (1974).

³C. Rosenzweig and G. F. Chew, Phys. Lett. 58B, 93 (1975).

⁴For a summary of work to date see P. Aurenche *et al.*, Rutherford Laboratory report, 1975 (unpublished).

⁵C. Schmid and C. Sorenson, Nucl. Phys. B96, 209 (1975).

⁶H. Harari, Phys. Rev. Lett. 22, 563 (1969).

⁷J. Rosner, Phys. Rev. Lett. 22, 689 (1969).

⁸Chan H.-Mo, J. E. Paton, Tsou S.-T., and Ng S.-W., Rutherford Laboratory Report No. RL-74-149, 1975 (unpublished); Nucl. Phys. B92, 13 (1975).

⁹C. Rosenzweig and G. Veneziano, Phys. Lett. 52B, 335 (1974).

¹⁰M. Schaap and G. Veneziano, Lett. Nuovo Cimento 12, 204 (1975).

¹¹H. Lee, Phys. Rev. Lett. 30, 719 (1973).

¹²G. Veneziano, Phys. Lett. 43B, 417 (1973).

¹³Chan H.-Mo and J. E. Paton, Phys. Lett. 46B, 228 (1973).

¹⁴The earliest suggestion that such diagrams should be associated with the Pomeron in dual models is by P. G. O. Freund and R. J. Rivers, Phys. Lett. 29B, 510 (1969).

¹⁵G. Frye and L. Susskind, Phys. Lett. 31B, 589 (1970).

¹⁶M. Ciafaloni, C. DeTar, and M. Mischeloff, Phys. Rev.

188, 2522 (1969).

¹⁷H. D. I. Abarbanel, Phys. Rev. D 6, 2788 (1972).

¹⁸J. Dash, Phys. Rev. D 9, 200 (1974) and further references cited in Ref. 19.

¹⁹N. Bali and J. Dash, Phys. Rev. D 10, 2102 (1974).

²⁰R. Carlitz, M. Green, and A. Zee, Phys. Rev. D 4, 3439 (1971); see also Refs. 21 and 22.

²¹P. G. O. Freund, H. F. Jones, and R. J. Rivers, Phys. Lett. 36B, 189 (1971).

²²C. Lovelace, Phys. Lett. 34B, 500 (1971).

²³*Dual Theory*, edited by M. Jacob (North-Holland, Amsterdam, 1974); P. H. Frampton, *Dual Resonance Models* (Benjamin, Reading, Mass., 1974).

²⁴P. G. O. Freund and Y. Nambu, Phys. Rev. Lett. 34, 1645 (1975).

²⁵G. F. Chew and D. Snider, Phys. Rev. D 1, 3453 (1970).

²⁶I. Iizuka, K. Okado, and O. Shito, Prog. Theor. Phys. 35, 1061 (1966).

²⁷S. Okubo, Phys. Lett. 5, 165 (1963).

²⁸G. Zweig, CERN Report No. 8419/TH 412, 1964 (unpublished).

²⁹F. E. Low, Phys. Rev. D 12, 163 (1975).

³⁰T. Appelquist and H. D. Politzer, Phys. Rev. Lett. 34, 43 (1975).

³¹J. Finkelstein, Nuovo Cimento 5A, 413 (1971).

³²G. F. Chew and J. Koplik, Nucl. Phys. B81, 93 (1974).

³³J. Dash and J. Koplik, Phys. Rev. D 12, 785 (1975).

³⁴R. E. Hendrick *et al.*, Phys. Rev. D 11, 536 (1975).

³⁵P. Stevens, private communication, California Institute of Technology (1975).

³⁶G. F. Chew and C. Rosenzweig, Lawrence Berkeley Laboratory Report No. LBL 4603, 1975 (unpublished).